Nozaki et al. *NPG Asia Materials* (2022) 14:5
https://doi.org/10.1038/s41427-021-00350-8

NPG Asia Materials

ARTICLE Open Access

Enhancing the interfacial perpendicular magnetic anisotropy and tunnel magnetoresistance by inserting an ultrathin LiF layer at an Fe/MgO interface

Takayuki Nozaki[1], Tomohiro Nozaki[1], Tatsuya Yamamoto[1], Makoto Konoto[1], Atsushi Sugihara[1], Kay Yakushiji[1], Hitoshi Kubota[1], Akio Fukushima[1] and Shinji Yuasa[1]

Abstract

Perpendicular magnetic anisotropy (PMA) is becoming increasingly important in spintronics research, especially for high-density magnetoresistive random access memories (MRAMs). The PMA induced at an Fe/MgO interface is widely used in magnetic tunnel junctions. Here, we propose inserting an ultrathin LiF layer at the interface in an epitaxial Fe/MgO junction. With a 0.3 nm-thick LiF layer, a large intrinsic interface PMA energy, $K_{i,0}$, of 2.8 mJ/m^2 was achieved. We also found that the LiF/MgO bilayer tunneling barrier exhibited a large tunnel magnetoresistance (TMR) effect, suggesting that a coherent spin-dependent tunneling process was maintained in the ultrathin LiF layer. Atomic-scale interface engineering using fluoride can further improve the PMA and TMR properties of spintronic devices.

Introduction

Magnetoresistive random access memories (MRAMs) are promising candidates for future nonvolatile memories. MgO-based magnetic tunnel junctions (MTJs), which consist of two ferromagnetic layers separated by an ultrathin MgO tunneling barrier, are essential memory elements in MRAMs[1,2]. Information is stored by controlling the magnetization direction in one of the two ferromagnetic layers (recording layer), while that in the other layer is fixed (reference layer). The tunneling conductance depends on the relative magnetization configuration between the two ferromagnetic layers, a phenomenon known as the tunnel magnetoresistance (TMR) effect, so that the magnetic information can be read out electrically.

Data retention in the recording layer is determined by the thermal stability factor, $\Delta = K_{\mathrm{PMA}}V/k_{\mathrm{B}}T$, where K_{PMA} is the effective perpendicular magnetic anisotropy (PMA) energy, V is the volume of the recording layer, k_{B} is the Boltzmann constant, and T is the temperature. Typically, $\Delta > 60$ is required to assure nonvolatility for the working memory. To maintain high thermal stability, a higher PMA is needed as the element size is reduced. Sufficiently high PMA can be obtained using bulk magnetic anisotropy, such as in $L1_0$-ordered (Co, Fe)−(Pt, Pd) alloys, (Co, Fe)/(Pt, Pd) multilayers, and rare-earth/transition-metal multilayers. However, these materials cannot be applied simply as a recording layer in MgO-based MTJs due to the band mismatch, which prevents coherent spin-dependent tunneling processes. Practically, PMA at the Fe-based alloy/MgO interface is employed to realize a perpendicular magnetic easy axis while maintaining a large TMR effect[3]. In an Fe/MgO heterostructure, the PMA at the interface originates from band hybridization between the $d_z{}^2$ orbital in the Fe and p_z orbitals in

Correspondence: Takayuki Nozaki (nozaki-t@aist.go.jp)
[1]National Institute of Advanced Industrial Science and Technology (AIST), Research Center for Emerging Computing Technologies, Tsukuba, Ibaraki 305-8568, Japan

oxygen;[4,5] therefore, the film thickness needs to be thin enough to overcome the demagnetization energy of the recording layer. Enhancement of the interface magnetic anisotropy is important to realize a high Δ value, not only for spin-transfer-torque MRAMs[6] but also for voltage-controlled MRAMs[7,8]. Several approaches have been proposed for the improvement in Δ utilizing the interface PMA, such as the introduction of a heavy metal buffer[9,10], a nitrogen-doped buffer[11], an MgO-double barrier structure[12,13], a spinel $MgAl_2O_4$ barrier[14], and heavy metal doping in a thin ferromagnetic layer[15,16].

In this work, we propose a new approach to enhance the interface PMA and TMR. This is done by introducing an ultrathin LiF layer at the Fe/MgO interface. Increases in the interface PMA using fluoride have been reported for polycrystalline Ta/CoFeB/AlF_3 and Ta/CoFeB/MgF_2 structures[17] compared with conventional oxide dielectric layers, such as Al_2O_3 and HfO_2; however, the TMR properties were not investigated. To realize both improved PMA and TMR properties, we focus on a LiF/MgO bilayer tunneling barrier. There have been a few reports of the TMR properties for structures with LiF tunneling barriers, both in experiments[18–20] and using first-principles calculations;[21] however, a large TMR effect has not yet been achieved at room temperature. Even for other fluoride materials, such as MgF_2, a large TMR effect has not yet been realized in MTJ structures[22,23], although their availability has been discussed in granular systems[24–26]. For this purpose, we prepared fully epitaxial Fe(001)/LiF (001)/MgO(001)/Fe(001) structures. Here, LiF/MgO works as a bilayer tunneling barrier. An enhancement of the interface PMA was confirmed when the ultrathin LiF layer was inserted between the ultrathin Fe and MgO. The intrinsic interface PMA energy, $K_{i,0}$, increased to 2.8 mJ/m^2, which is approximately 1.4 times larger than that of a standard Fe/MgO interface (2.0 mJ/m^2). We also observed an increase in the TMR ratio when LiF was inserted, suggesting that a coherent tunneling process was maintained in the LiF/MgO bilayer.

Materials and methods

Figure 1a shows a schematic illustration of the sample structure, which is a multilayer stack consisting of a Cr/Fe wedge ($t_{Fe} = 0$–1.0 nm)/LiF wedge ($t_{LiF} = 0$–0.3 nm)/MgO (2.3 nm)/top electrode grown on an MgO(001) substrate by a combination of molecular beam epitaxy and sputtering techniques. A 5 nm-thick MgO(001) seed layer and a 30 nm-thick Cr(001) buffer layer were deposited at 200 °C followed by annealing at 800 °C. An ultrathin Fe(001) layer was grown at 150 °C and annealed at 250 °C. After the substrate temperature was lowered to room temperature, ultrathin LiF(001) and MgO (001) layers were deposited followed by annealing at 250 °C. The MgO surface was capped with a sputter-deposited 20 nm-thick ITO electrode (device A) for evaluation of the magnetic properties by polar-MOKE measurements. For the STEM observations and TMR measurements, a 10 nm-thick Fe reference layer (device B) was deposited on the MgO(001) tunneling barrier at a substrate temperature of 200 °C followed by annealing at 250 °C. Finally, the top Fe layer was covered by sputter-deposited Ta (5 nm)/Ru (7 nm) capping layers. MTJ devices were prepared by conventional optical lithography, ion-milling, and lift-off processes. The cross-sectional area of the junction was designed to be 2×6 μm^2. The TMR curves were measured with a conventional direct-current two-probe method under the application of in-plane magnetic fields at room temperature.

Results and discussion

Epitaxial growth of LiF(001) on Fe(001) and MgO(001) on LiF(001) was confirmed by reflection high-energy electron diffraction (RHEED) with sharp streaks, as shown in Fig. 1b, c. Here, the incident electron beam is parallel to the [100] azimuth of the MgO substrate. The lattice constant of LiF ($a = 0.402$ nm) is smaller than that of MgO ($a = 0.421$ nm) and matches well with that of Fe ($a = 0.286$ nm) when it is rotated by 45° ($\sqrt{2}a = 0.404$ nm). Single crystal lattices with flat interfaces were also confirmed by high-angle annular dark-field scanning transmission electron microscopy (HAADF-STEM) imaging (Fig. 1d). For the STEM observation, we used an MTJ structure with a thicker LiF layer consisting of Cr/Fe(0.7 nm)/LiF(0.4 nm)/MgO(2.3 nm)/Fe (10 nm) to monitor the concentration distribution of fluorine (F) more clearly. Figure 1e shows the intensity profiles of electron energy-loss spectroscopy (EELS) of oxygen (O), fluorine (F), magnesium (Mg), chromium (Cr), and iron (Fe). We can see a clear fluorine peak between the Fe and MgO layers. There may be some finite intermixing at the LiF/MgO interface due to the smaller signals of Mg and O in the LiF layer; however, we can expect that the interface PMA properties, as discussed below, might be dominated by the Fe/LiF interface.

The Fe thickness dependencies of the polar MOKE hysteresis curves for device A are shown in Fig. 2. The LiF thicknesses, $t_{LIF,}$ were designed to be (a) 0 nm, (b) 0.1 nm, (c) 0.2 nm and (d) 0.3 nm. For the standard Fe/MgO structure, we observed a transition of the magnetic easy axis from perpendicular to in-plane at approximately $t_{Fe} = 0.66$ nm. On the other hand, with the LiF layer, an increase in the transition thickness was observed with an enlargement in the coercivity. The perpendicular magnetic easy axis was maintained even at approximately $t_{Fe} = 0.8$ nm for the case with $t_{LiF} = 0.3$ nm, as shown in Fig. 2d, indicating an enhancement in the PMA.

For a detailed quantitative evaluation of the PMA energy, we prepared orthogonally magnetized MTJ structures (device B), which have a perpendicularly magnetized ultrathin Fe layer sandwiched between Cr and LiF

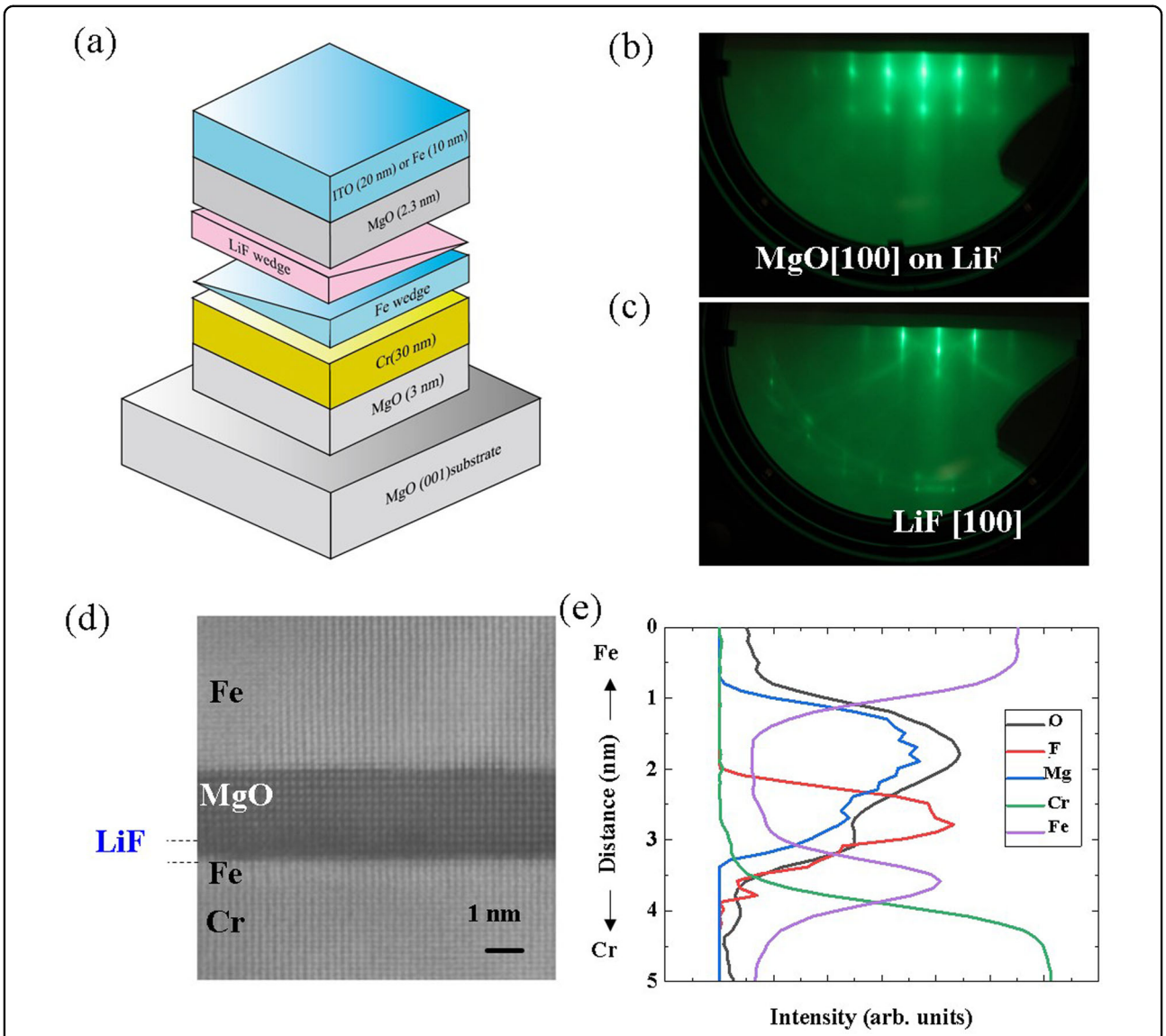

Fig. 1 Magnetic tunnel junction with a LiF/MgO bilayer tunnel barrier. a Schematic of the prepared heterostructures consisting of a Cr(30 nm)/Fe wedge ($t_{Fe} = 0$–1.0 nm)/LiF wedge ($t_{LiF} = 0$–0.3 nm)/top electrode grown on a MgO(001) substrate. RHEED patterns for **b** MgO[100] grown on LiF and **c** LiF[100] grown on Fe. **d** Cross-sectional HAADF-STEM image and **e** EELS intensity profiles across the interface for each atomic species in the Cr/Fe(0.6 nm)/LiF(0.4 nm)/MgO(2.3 nm)/Fe(10 nm) structure.

(or MgO) and an in-plane magnetized Fe layer of 10 nm as a top reference layer. Application of an in-plane magnetic field (H_{ex}) tilts the magnetization of the free layer in the film plane, while that of the reference layer stays in the film plane, as illustrated in Fig. 3a. Therefore, we can evaluate the magnetization process of the free layer in the magnetic hard axis direction under in-plane magnetic fields. The LiF thickness dependence of the TMR curves is shown in Fig. 3a for a fixed Fe thickness of 0.5 nm. Here, the vertical axis is normalized by the maximum ($H_{ex} =$ 0 Oe) and minimum ($H_{ex} = 40$ kOe) resistances to avoid the influence of the bias voltage dependence of the TMR ratio. The saturation property of the TMR curves reflects the perpendicular anisotropy fields for the ultrathin Fe layer. With increasing LiF thickness, a systematic increase in the saturation field is observed. This tendency is consistent with that observed in the polar-MOKE measurements. With LiF layers thicker than 0.2 nm, the saturation fields reach up to 30 kOe, which is approximately twice that of a standard Fe/MgO MTJ.

From these TMR curves, we can calculate the effective PMA energy, K_{PMA}, for each Fe thickness using the following evaluation process:[27] Since the tunneling conductance depends on the relative angle, θ between the two

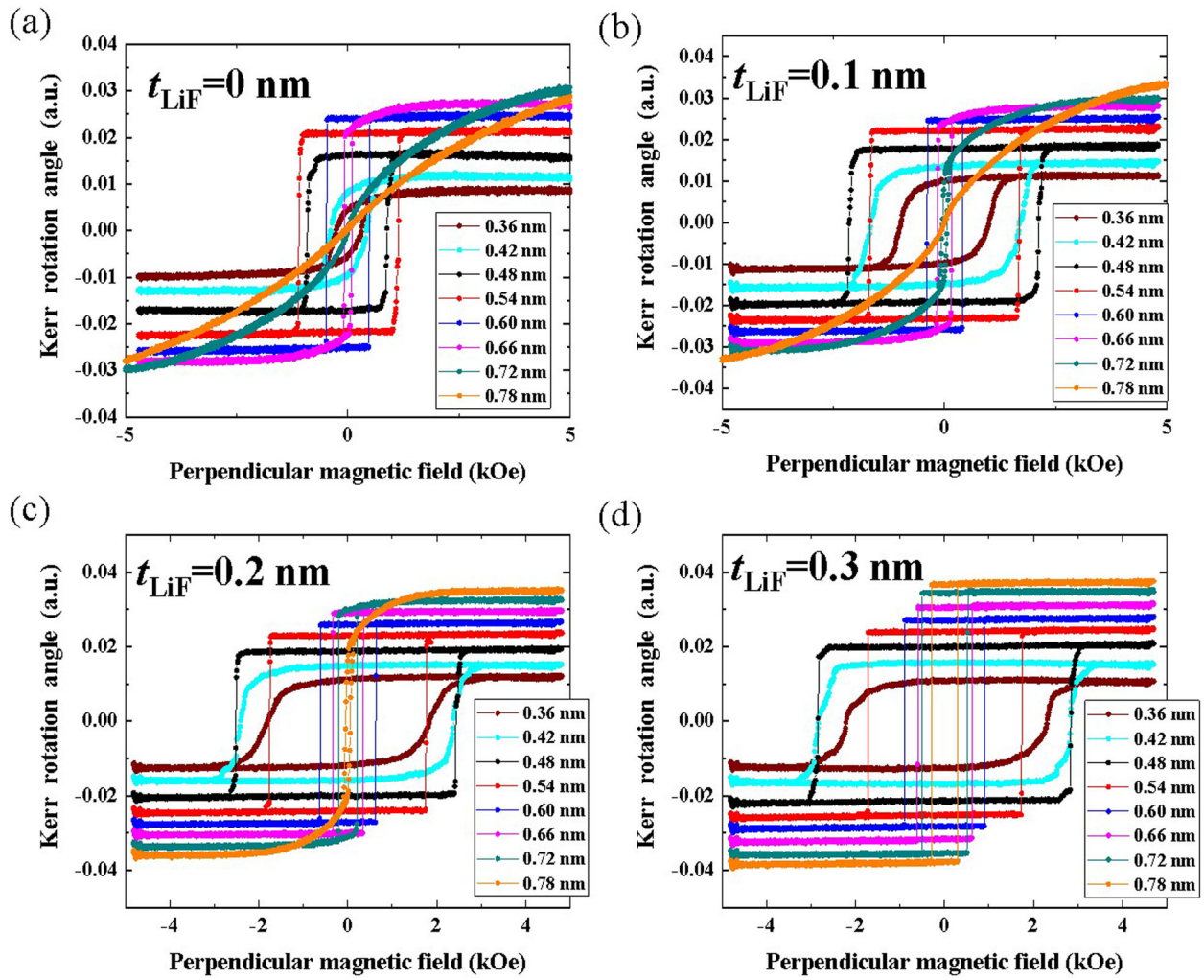

Fig. 2 Influence of LiF layer insertion at the interface on the magnetic hysteresis curves of an ultrathin Fe layer. Fe thickness dependence of polar-MOKE hysteresis curves for structures **a** without LiF, with **b** $t_{LiF} = 0.1$ nm, **c** $t_{LiF} = 0.2$ nm, and **d** $t_{LiF} = 0.3$ nm.

ferromagnetic layers, the ratio of the in-plane component of the magnetization for the ultrathin Fe layer, $M_{\text{in-plane}}$ to the saturation magnetization, M_S is calculated from the following relationship:

$$\frac{M_{\text{in-plane}}}{M_S} = \cos\theta = \frac{R_{90} - R(\theta)}{R(\theta)} \frac{R_P}{R_{90} - R_P} \quad (1)$$

where R_P and R_{90} are the MTJ resistances in the parallel and orthogonal configurations, respectively. $R(\theta)$ is the MTJ resistance when the magnetization of the Fe free layer is tilted toward the in-plane direction at angle θ from the film plane by the application of an in-plane magnetic field. K_{PMA} can be evaluated by calculating the area above the normalized $M_{\text{in-plane}}/M_S$ (H_{ex}) curve with the M_S value obtained by other measurements (shaded area in the inset of Fig. 3c). By using the wedge-shaped MTJ, we can perform a systematic evaluation of K_{PMA} as a function of the Fe and LiF thicknesses. The saturation magnetization, M_S, was independently measured using a vibrating-sample magnetometer (VSM). Figure 3b shows the Fe thickness dependence of the magnetic moment for Cr/Fe(t_{Fe})/LiF (0.2 nm)/MgO(2.3 nm)/ITO structures with a sample size of 1 cm × 2 cm. A linear increase in the magnetic moment was confirmed with increasing t_{Fe}. A distinct magnetic dead layer was not observed in this structure. The value of M_S was evaluated to be approximately 2.0 T, which is comparable to that of a standard Cr/Fe/MgO structure, as shown by the red star in Fig. 3b. These results imply that a pure ultrathin Fe layer is maintained at the Fe/LiF interface even after a post-annealing process.

Figure 3c presents the dependence of $K_{PMA}t_{Fe}$ on the Fe thickness for different tunneling barriers consisting of a single MgO (2.5 nm) layer and LiF (0.1–0.3 nm)/MgO

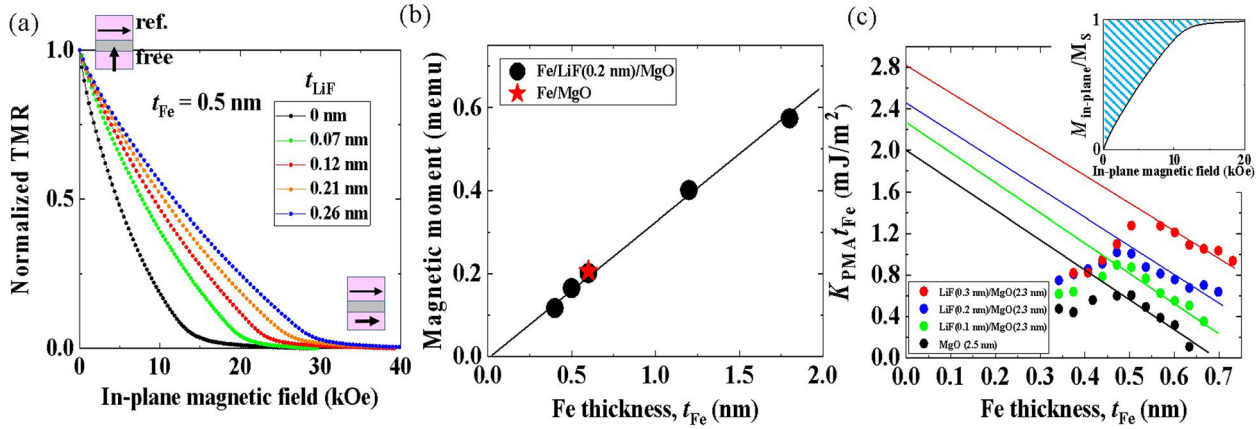

Fig. 3 Evaluation of the interface perpendicular magnetic anisotropy in MTJ structures. a The LiF thickness, t_{LiF}, dependence of normalized TMR curves measured under an in-plane magnetic field with a fixed Fe thickness of $t_{Fe} = 0.5$ nm. **b** Nominal Fe thickness dependence of the magnetic moment for the sample with $t_{LiF} = 0.2$ nm (sample size: 1 cm × 2 cm). No clear degradation in the magnetic moment was observed even in the ultrathin Fe thickness region ($t_{Fe} < 1.0$ nm). The red star shows reference data obtained in a standard Fe/MgO structure. **c** $K_{PMA}t_{Fe}$ as a function of Fe thickness for MTJs with different barrier structures consisting of a single MgO layer (black dots), LiF(0.1 nm)/MgO layers (green dots), LiF(0.2 nm)/MgO layers (blue dots), and LiF(0.3 nm)/MgO layers (red dots). Linear fitting was conducted to evaluate the $K_{i,0}$ value in the thick Fe region, where a linear relation was observed, as shown by solid lines. The inset shows an example of a normalized $M_{in\text{-}plane}$ (H_{ex}) curve obtained from the TMR curve for the MTJ with $t_{Fe} = 0.52$ nm and without a LiF layer.

(2.3 nm) bilayers. The effective magnetic anisotropy energy, K_{PMA}, can be expressed by the following phenomenological expression:

$$K_{PMA} = \left(K_V - \frac{1}{2}\mu_0 M_S^2\right) + \frac{K_{i,0}}{t_{Fe}} \quad (2)$$

where K_V and μ_0 are the volume anisotropy and vacuum permeability, respectively. $K_{i,0}$ represents the intrinsic interface PMA, which can be evaluated from the intercept in a plot of $K_{PMA}t_{Fe}$ versus t_{Fe}. The expected linear relationship was confirmed for $t_{Fe} > 0.5$ nm, whereas a reduction in $K_{PMA}t_{Fe}$ occurred in the thinner Fe thickness regions. This trend is consistent with the Fe thickness dependence of the coercivity change observed in Fig. 2. The possible origin of the deviation may relate to the magnetoelastic effect, as discussed in previous works[28,29]. $K_{i,0}$ is the representative value expressing the amplitude of interface magnetic anisotropy at zero Fe thickness. For the standard Fe/MgO interface, the $K_{i,0}$ value was evaluated to be approximately 2.0 mJ/m^2 from the linear fitting in the thicker t_{Fe} region. This is comparable to the previously reported values[29,30]. $K_{i,0}$ is enhanced systematically by inserting a LiF layer and reaches approximately 2.8 mJ/m^2 at $t_{LiF} = 0.3$ nm. A similar enhancement in the PMA was also observed when other fluoride materials, such as MgF_2 and CaF_2, were inserted (not shown here). Therefore, the origin of the improved PMA seems to come from the band hybridization between Fe and fluorine. However, we could not obtain a large TMR effect when MgF_2 or CaF_2 layers were inserted at the Fe/MgO interface. On the other hand, LiF is a suitable material even from the viewpoint of the TMR properties, as discussed next. For K_V, all structures show almost the same values of approximately −0.5 MJ/m^3, which is comparable to that observed in the standard Fe/MgO[15]. This suggests that LiF insertion has little influence on the volume anisotropy.

Figure 4a shows the LiF thickness dependence of the tunneling resistance in a parallel magnetization configuration (red dots). Here, the Fe thickness is fixed at 0.54 nm. An exponential increase in the resistance is observed, indicating that the LiF layer also works as an additional tunneling barrier. The rate of increase in the resistance is larger than that of a single MgO barrier (shown by black dots in Fig. 4a), probably due to the larger energy band gap of LiF (8.7 eV) compared to that of MgO (7.8 eV).

The LiF and MgO thickness dependence of the TMR ratio is shown in Fig. 4b. Here, the vertical axis represents half of the full TMR ratio due to the orthogonal magnetization configuration in our MTJs. For the standard Fe/MgO MTJ, the TMR ratio decreases gradually and reaches a minimum at an MgO thickness of approximately 0.15 nm; however, it recovers again with increasing MgO thickness. This trend may come from the oscillatory variation in TMR as a function of MgO thickness reported in the previous work[1]. Interestingly, the LiF/MgO bilayer MTJ shows the opposite trend, i.e., the TMR ratio increases gradually and reaches a maximum at a LiF thickness of approximately 0.15 nm, followed by a decrease with increasing LiF thickness. In the LiF thickness ranges investigated in this work, the TMR ratios are

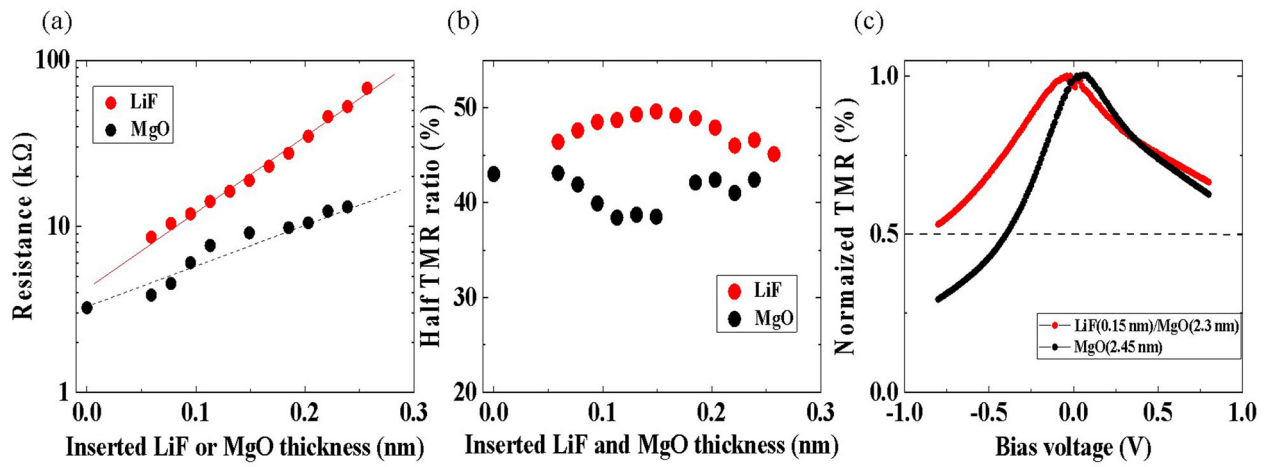

Fig. 4 Influence of the LiF layer insertion on the TMR properties. LiF and MgO thickness dependencies of **a** tunneling resistance in a parallel magnetization configuration and **b** TMR ratio for the MgO(t_{MgO})/MgO(2.3 nm) layers (black dots) and LiF(t_{LiF})/MgO(2.3 nm) layers (red dots), respectively. **c** Comparison of bias voltage dependence of normalized TMR ratio for the MTJs with an MgO(2.45 nm) barrier (black dots) and a LiF (0.15 nm)/MgO(2.3 nm) bilayer barrier (red dots).

basically larger than that of the Fe/MgO standard structure. We need further investigation over a wider range of LiF thicknesses to investigate the physical origin of the observed tendency; nevertheless, we can at least conclude that the coherent tunneling process of the Δ_1 band in the Fe(001) electrode is maintained even in the ultrathin LiF (001) layer as well as at the MgO(001) barrier, which can provide a large TMR effect.

The bias voltage dependence of the TMR for two types of tunneling barriers is compared for structures with a single MgO (2.45 nm) layer and a LiF (0.15 nm)/MgO (2.3 nm) bilayer in Fig. 4c. The MgO single barrier exhibits an asymmetric bias voltage dependence (black dots), as observed in the previous report[1]. At negative bias voltages, where it is sensitive to the electronic structure at the bottom Fe/MgO interface, the bias voltage at which the TMR ratio becomes half of the maximum value is approximately half that in the positive bias voltage direction. The cause of this degradation can be explained by structural defects, such as dislocations and lattice distortions[31]. On the other hand, the bias voltage dependence is relatively symmetric when an ultrathin LiF layer is inserted at the interface (red dots). This tendency can be explained by an improvement in the lattice matching at the Fe/LiF interface, similar to that discussed in Fe/$MgAl_2O_4$ MTJs[31].

Conclusion

In summary, the effect of inserting an ultrathin LiF layer at the Fe/MgO interface on the PMA and TMR properties of an MTJ structure was investigated. With a LiF layer, the interface PMA was enhanced with a large $K_{i,0}$ value of approximately 2.8 mJ/m^2. We also observed a large TMR through the LiF/MgO bilayer tunneling barrier, suggesting that the coherent tunneling process of the Δ_1 band was maintained in the LiF layer. Interface engineering using an ultrathin LiF layer is a new approach to developing MTJs with high thermal stability while maintaining a large TMR effect.

Acknowledgements

This work was partly based on results obtained from a project, JPNP16007, commissioned by the New Energy and Industrial Technology Development Organization (NEDO), Japan. The authors thank M. Endo, H. Ohmori, Y. Sato, Y. Kageyama, L. Sakai, K. Hiraga, Y. Higo, and M. Hosomi of the Sony Semiconductor Solutions Corporation, S. Miwa and S. Sakamoto of the Univ. of Tokyo, and H. Imamura, Y. Kitaoka, T. Taniguchi, and Y. Hibino of AIST for their fruitful discussions.

Author contributions

T.N. planned and performed the sample fabrication, measurement, and data analysis. T.N., M.K., T.Y, A.S., K.Y., H.K., A.F., and S.Y. developed techniques for deposition, microfabrication, and measurements. T.N. wrote the manuscript with review and input from T.N., M.K., T.Y, A.S., K.Y., H.K., and A.F. S.Y. planned and supervised the project. All authors contributed to the planning, discussion, and analysis of this research.

Conflict of interest

The authors declare no conflict of interest.

Received: 9 August 2021 Revised: 4 December 2021 Accepted: 14 December 2021.
Published online: 28 January 2022

References

1. Yuasa, S., Nagahama, T., Fukushima, A., Suzuki, Y. & Ando, K. Giant room-temperature magnetoresistance in single-crystal Fe/MgO/Fe magnetic tunnel junctions. *Nat. Mater.* **3**, 868–871 (2004).

2. Parkin, S. S. et al. Giant tunnelling magnetoresistance at room temperature with MgO (100) tunnel barriers. *Nat. Mater.* **3**, 862–867 (2004).
3. Ikeda, S. et al. A perpendicular-anisotropy CoFeB–MgO magnetic tunnel junction. *Nat. Mater.* **9**, 721–724 (2010).
4. Yang, H. X. et al. First-principles investigation of the very large perpendicular magnetic anisotropy at Fe|MgO and Co|MgO interfaces. *Phys. Rev. B* **84**, 054401 (2011).
5. Okabayashi, J. et al. Perpendicular magnetic anisotropy at the interface between ultrathin Fe film and MgO studied by angular-dependent X-ray magnetic circular dichroism. *Appl. Phys. Lett.* **105**, 122408 (2014).
6. Ikeda, S. et al. Recent progress of perpendicular anisotropy magnetic tunnel junctions for nonvolatile VLSI. *Spin* **02**, 1240003 (2012).
7. Amiri, P. K. et al. Electric-Field-Controlled Magnetoelectric RAM: Progress, Challenges, and Scaling. *IEEE Trans. Magn.* **51**, 3401507 (2015).
8. Nozaki, T. et al. Recent progress in the voltage-controlled magnetic anisotropy effect and the challenges faced in developing voltage-torque MRAM. *Micromachines* **10**, 327 (2019).
9. Worledge, D. C. et al. Spin torque switching of perpendicular Ta|CoFeB|MgO-based magnetic tunnel junctions. *Appl. Phys. Lett.* **98**, 022501 (2011).
10. Pai, S.-F. et al. Enhancement of perpendicular magnetic anisotropy and transmission of spin-Hall-effect-induced spin currents by a Hf spacer layer in W/Hf/CoFeB/MgO layer structures. *Appl. Phys. Lett.* **104**, 082407 (2014).
11. Sinha, J. et al. Enhanced interface perpendicular magnetic anisotropy in Ta|CoFeB|MgO using nitrogen-doped Ta underlayers. *Appl. Phys. Lett.* **102**, 242405 (2013).
12. Sato, H. et al. Perpendicular-anisotropy CoFeB—MgO magnetic tunnel junctions with a MgO/CoFeB/Ta/CoFeB/MgO recording structure. *Appl. Phys. Lett.* **101**, 022414 (2012).
13. Kubota, H. et al. Enhancement of perpendicular magnetic anisotropy in FeB free layers using a thin MgO cap layer. *J. Appl. Phys.* **111**, 07C723 (2012).
14. Xiang, Q., Mandal, R., Sukegawa, H., Takahashi, Y. K. & Mitani, S. Large perpendicular magnetic anisotropy in epitaxial Fe/MgAl2O4(001) heterostructures. *Appl. Phys. Exp.* **11**, 063008 (2018).
15. Nozaki, T. et al. Highly efficient voltage control of spin and enhanced interfacial perpendicular magnetic anisotropy in iridium-doped Fe/MgO magnetic tunnel junctions. *NPG Asia Mater.* **9**, e451–e451 (2017).
16. Nozaki, T. et al. Enhancement in the interfacial perpendicular magnetic anisotropy and the voltage-controlled magnetic anisotropy by heavy metal doping at the Fe/MgO interface. *APL Mater.* **6**, 026101 (2018).
17. Pankieiev, M. & Kita, K. Effects of oxide replacement with fluoride at the CoFeB interface on interface magnetic anisotropy and its voltage control. *AIP Adv.* **8**, 055901 (2018).
18. Xue, Q. et al. Tunnel magnetoresistance in epitaxial (100)-oriented FeCo/LiF/FeCo magnetic tunnel junctions. *Appl. Phys. Lett.* **109**, 192407 (2016).
19. Narayananellore, S. K., Doko, N., Matsuo, N., Saito, H. & Yuasa, S. Fabrication of magnetic tunnel junctions with a single-crystalline LiF tunnel barrier. *Jpn. J. Appl. Phys.* **57**, 04FN04 (2018).
20. Liu, F. et al. Resonant TMR inversion in LiF/EuS based spin-filter tunnel junctions. *AIP Adv.* **6**, 085004 (2016).
21. Vlaic, P., Burzo, E. & Carva, K. Are insulating LiF barriers relevant for spin-polarized tunnelling applications? Insights from first-principles calculations. *J. Phys. D: Appl. Phys.* **49**, 305302 (2016).
22. Mitani, S., Moriyama, T. & Takanashi, K. Structure and tunnel magnetoresistance in Fe/MgF[sub 2]/Co junctions with an oxide seed layer on an Fe bottom electrode. *J. Appl. Phys.* **91**, 7200 (2002).
23. Harada, K., Makabe, K. S., Akinaga, H. & Suemasu, T. Room temperature magnetoresistance in $Fe_3Si/CaF_2/Fe_3Si$ MTJ epitaxially grown on Si(111). *J. Phys.: Conf. Ser.* **266**, 012088 (2011).
24. Furubayashi, T. & Nakatani, I. Giant magnetoresistance in granular Fe–MgF2 films. *J. Appl. Phys.* **79**, 6258 (1996).
25. Kobayashi, N., Ohnuma, S., Masumoto, T. & Fujimori, H. (Fe–Co)–(Mg-fluoride) insulating nanogranular system with enhanced tunnel-type giant magnetoresistance. *J. Appl. Phys.* **90**, 4159–4162 (2001).
26. Ono, K et al. Electrical Conduction and Tunneling Magnetoresistance of Fe,Co/MgF_2 Granullar Multilayers. *Jpn. J. Appl. Phy.* **41**, 97–102 (2002).
27. Shiota, Y. et al. Quantitative evaluation of voltage-induced magnetic anisotropy change by magnetoresistance measurement. *Appl. Phys. Exp.* **4**, 043005 (2011).
28. Bloemen, P. J. H., Johnson, M. T., den Broeder, F. J. A. & de Vries, J. J. Magnetic anisotropy in metallic multilayers. *Rep. Prog. Phys.* **59**, 1409–1458 (1996).
29. Nozaki, T. et al. Large voltage-induced changes in the perpendicular magnetic anisotropy of an MgO-based tunnel junction with an ultrathin Fe Layer. *Phys. Rev. Appl.* **5**, 044006 (2016).
30. Koo, J. W. et al. Large perpendicular magnetic anisotropy at Fe/MgO interface. *Appl. Phys. Lett.* **103**, 192401 (2013).
31. Sukegawa, H. et al. Tunnel magnetoresistance with improved bias voltage dependence in lattice-matched Fe/spinel MgAl2O4/Fe(001) junctions. *Appl. Phys. Lett.* **96**, 212505 (2010).